Journal of the Korean Nuclear Society
Volume 32, Number 1, pp.46~56, February 2000

A Numerical Analysis on the Transient Heat Transfer in a Heat Exchanger Pipe Flow

Keun Sun Chang and Young Chel Kweon
Sun Moon University
Asan Choongnam 336-840, Korea
chang@omega.sunmoon.ac.kr

Seong Ryung Jin
Korea Power Engineering Co.
150 Dukjin-dong Yusong-gu, Taejon 305-353, Korea

(Received August 11, 1999)

Abstract

Numerical results are presented for the 2-dimensional turbulent transient heat transfer of the shell/tube heat exchanger with a step change of the inlet temperature in the primary side. Heat transfer boundary conditions outside the pipe are given partially by the convection heat transfer conditions and partially by insulated conditions. Calculation results were obtained by solving the unsteady two-dimensional elliptic forms for the Reynolds-averaged governing equations for the mass, momentum and energy. Finite-difference method was used to obtain discretization equations, and the SIMPLER solution algorithm was employed for the calculation procedure. Turbulent model used is the algebraic model proposed by Cebeci-Smith. Results presented include the time variant Nusselt number distribution, average temperature distribution and outlet temperatures for the various inlet temperatures and flow rates.

Key Words : transient heat transfer, internal flow, shell/tube heat exchanger, Nusselt number

1. Introduction

Unsteady forced convection heat transfer in internal flows is widely encountered in the control problem of modern high performance heat transfer devices such as power plants, aerospace equipments, and chemical processes. Particularly, the transient heat transfer problem in a heat exchanger of the nuclear power plants is very important in the case of switchover between a operating mode and stop mode. The reactor coolant pump seal injection water in pressurized water reactors is controlled by CVCS seal injection system within a certain range of temperature in order to maintain the seal integrity for the design life time. During transients such as switchover of seal injection water source from the high temperature of volume control tank to the low

Table 1. Conservation Equations

Conserved Property	Φ	Γ_ϕ	S_ϕ
Mass	1	0	0
x-Momentum	U	μ_{eff}	$\frac{\partial}{\partial x}\left(\mu_{eff}\frac{\partial U}{\partial x}\right)+\frac{1}{r}\frac{\partial}{\partial r}\left(r\mu_{eff}\frac{\partial V}{\partial r}\right)-\frac{\partial P}{\partial x}$
r-Momentum	V	μ_{eff}	$\frac{\partial}{\partial x}\left(\mu_{eff}\frac{\partial U}{\partial r}\right)+\frac{1}{r}\frac{\partial}{\partial r}\left(r\mu_{eff}\frac{\partial V}{\partial x}\right)-2\mu_{eff}\frac{V}{r^2}-\frac{\partial P}{\partial r}$
Energy	T	$\rho\Gamma_{eff}$	0

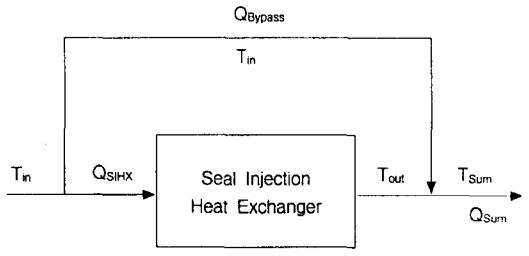

Fig. 1. Schematic Diagram of Bypass Line

temperature of refueling water storage tank, there is quite a possibility of severe seal injection water temperature variation. Since operating reactors(for example, YGN 3&4 and UCN 3&4) have experienced a number of operating conditions which exceed design requirements for the seal injection temperature range or temperature variation limit, necessity of a design improvement has been recognized.

In this study, in order to understand the transient heat transfer on the seal injection temperature variation, the flow rate through the seal injection heat exchanger is controlled with respect to the inlet temperature variation by installing bypass line around the heat exchanger(Fig. 1). Also, operation characteristics of the seal injection heat exchanger are analyzed to predict design parameters such as the bypass flow rate and seal injection temperature for various inlet flow rates and temperatures. A numerical technique is utilized to investigate the flow and heat transfer characteristics of the seal injection heat exchanger. Calculation results are obtained by solving the unsteady two-dimensional time-averaged conservation equations for the mass, momentum and energy. Finite-difference procedure is employed for the calculation procedure, and solutions are obtained iteratively using the SIMPLER algorithm[1].

For the first approximation of transient convection heat transfer, it is common practice to prescribe the wall temperature, the wall heat flux, or a combination of the two at the solid-fluid interface. However, in reality, the boundary conditions cannot be known a priori; rather they depend on the coupled mechanism of convection heat transfer in the fluid and conduction in the solid. The simplest approach to the transient convection heat transfer problem is to assume an extremely thin wall so that effects of thermal capacity and resistance of the wall can be neglected[2-4]. Cotta et al.[4] proposed a second-order accurate finite-difference scheme for the channel flow with a step change in inlet temperature.

The influence of heat capacity of a duct wall on transient forced convection heat transfer in channels and pipes has been studied by Sucec[5] and Sucec and Sawant[6] with the assumption that

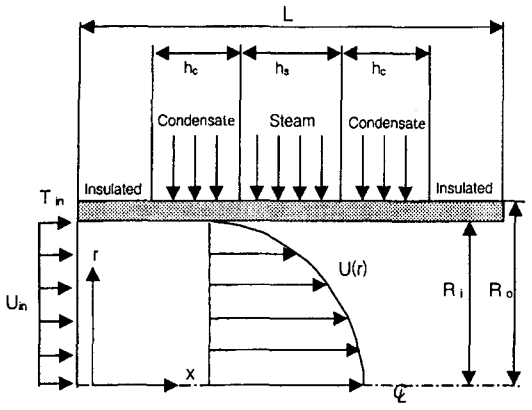

Fig. 2. Geometric Model of Flow Field

a lumped system in the pipe is subjected to an insulated boundary condition. Sucec[7] developed a system for the finite thermal capacity walls that transfer energy with an ambient environment. Lin and Kuo[8] were the first investigators to study the problem of transient conjugated heat transfer including the effect of heat conduction in the pipe wall. Lee and Yan[9] studied the effects of wall thickness, wall-to-fluid conductivity and diffusivity ratios for fully developed laminar transient conjugated forced convection using the finite-difference technique. However, there are still lack of information on unsteady forced heat transfer in duct subjected to a step change in inlet temperature.

2. Calculation Method

2.1. Governing Equations

The seal injection heat exchangers (YGN 3&4 and UCN 3&4) are consist of a bundle of shell/tube with 10 U-tubes. In this study, one straight tube is analyzed with the assumption that physical parameters and heat transfer characteristics in each tube are identical(Fig. 2). The heat transfer characteristics may be different with the actual case when the U-bend region is assumed with the straight one. The velocity oc outward region of U-bend is higher than inward region and vortex flow is formed around the U-bend. However, since the length of U-bend with respect to the overall length of the tube is relatively short, U-bend effects is negligible.

As shown in Fig. 2, secondary boundary conditions of the tube are specified with 5 distinguished regions which are consistent with the actual operating conditions of the seal injection heat exchanger with the two lower tube sheet regions at both ends of the tube(insulated condition), two condensate regions and a steam region in the middle. At the initial state, the fluid velocity at x=0 is uniform(U_{in}), but, the inlet temperature is instantly changed from the intial temperature to the inlet temperature of Tin. In this case, heat transfer at the wall occurs through both upstream and downstream directions due to conduction, and the heat transfer at the wall-fluid interface occurs in the radial direction through the convective mechanism. In the fluid region, heat is transferred to the flow direction due to fluid conduction and convection and heat is also transferred to the reverse direction due to the axial conduction from the wall.

The calculation domain is selected to analyze the transient heat transfer characteristics in the tube of length L and radius D, as shown in Fig. 2. Investigation is made for various inlet flow rates and inlet temperatures. The flow is symmetric with respect to the plane passing through the center of the tube. Therefore, the solution domain is the half of the tube, bounded by the symmetry axis and walls.

The flow is assumed to be incompressible, unsteady two-dimensional turbulent. The temperature and the velocity components obey the turbulent time-averaged continuity, momentum and energy equations. The thermo-physical

properties of the fluids are assumed to be constant and the gravity effect is neglected. With these assumptions and flow conditions, solutions can be sought for a set of elliptical partial differential transport equations that all have the general form in the cylindrical coordinate as:

$$\rho\frac{\partial\Phi}{\partial t}+\frac{\partial}{\partial x}(\rho U\Phi)+\frac{1}{r}\frac{\partial}{\partial r}(r\rho V\Phi) = \frac{\partial}{\partial x}\left(\Gamma_\Phi\frac{\partial\Phi}{\partial x}\right)+\frac{1}{r}\frac{\partial}{\partial r}\left(r\Gamma_\Phi\frac{\partial\Phi}{\partial r}\right)+S_\Phi \quad (1)$$

where Φ is the general dependent variable such as U, V, T, and Γ_Φ is the general form of diffusion coefficients, and S_Φ is the source term which include all terms except the convection and diffusion terms. The quantities, Γ_Φ and S_Φ are specific to a particular dependent variable of Φ. The definition of Γ_Φ and S_Φ is presented in Table 1.

The effective viscosity μ_{eff} and thermal diffusion coefficient Γ_Φ are the sum of the molecular and turbulent contributions:

$$\mu_{eff} = \mu + \mu_t \quad (2)$$

$$\Gamma_{eff} = \alpha + \frac{\mu_t}{\mathrm{Pr}_t} \quad (3)$$

where α is the thermal diffusivity and Pr_t is the turbulent Prandtl number with a value of 0.9. The algebraic turbulent model of Cebeci-Smith[10] is used to express the turbulent viscosity in this study. The model is a two-layer model with μ_t given by separate expression in each layer:

Inner layer

$$\mu_t=\rho\, l_{mix}^2\left[\left(\frac{\partial U}{\partial r}\right)^2+\left(\frac{\partial V}{\partial x}\right)^2\right]^{1/2} \quad (4)$$

with $l_{mix}=k r\left[1-e^{-r^+/A^+}\right]$

Outer layer

$$\mu_t=\alpha\rho U_e\,\delta_v^*\,F_K \quad (5)$$

with closure Coefficients:

$$k=0.41,\quad \alpha=0.0168,$$

$$A^+=26\left[1+r\frac{dP/dx}{\rho\, u_\tau^2}\right]^{-1/2}$$

In Eq. (5), U_e is boundary-layer edge velocity, δ_v is the velocity thickness and u_τ is the friction velocity. The function F_K is the Klebanoff intermittency function given by:

$$F_K=\left[1+\left(\frac{r}{\delta}\right)\right]^{-1} \quad (6)$$

The turbulent model is relatively simple, but is known to be accurate for wall-bounded flows such as channel and pipe flows.

2.2. Boundary and Initial Conditions

Since the set of partial differential flow equation is parabolic in time and elliptic in space, it is necessary to define initial and boundary conditions for all variables on all boundaries of the flow domain. At the inlet, all dependent variables are prescribed as given by design values, while zero gradients of all of the dependent variables in the x direction are set at the outlet (a fully developed condition). At the initial state, the fluid velocity at x = 0 is uniform(U_{in}), but, the inlet temperature is instantly changed from the intial uniform temperature to inlet temperature T_{in}. Outside wall boundary conditions of the tube are specified with constant heat transfer coefficients for 5 distinguished regions as shown in Fig. 2 and then the boundary condition at inner wall-fluid interface is calculated using the continuity condition of heat flux and temperature at the interface and energy balance at the wall, i.e.:

at $r=R_i$,

$$U(T_{sec}-T)=-k\left(\frac{\partial T}{\partial r}\right)+\rho_w c_{pw} b\frac{\partial T}{\partial t} \quad (7)$$

where T_{sec} is the secondary temperature, and ρ_w, c_{pw} and b are the density, specific heat and thickness of the wall, respectively, and U is the combined heat transfer coefficient of

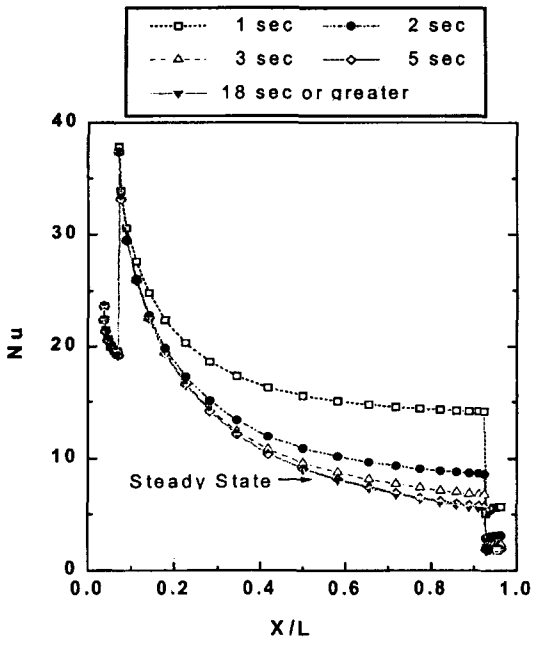

Fig. 3. Axial Distribution of Nusselt Number for Various Time Steps with Tin=40°F

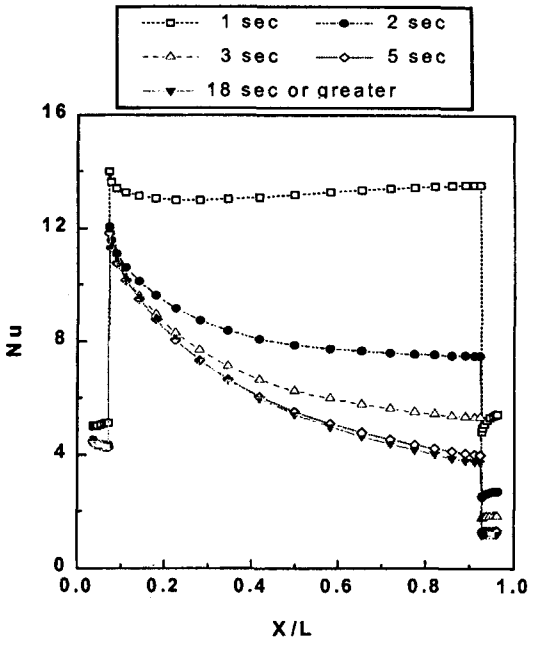

Fig. 4. Axial Distribution of Nusselt Number for Various Time Steps with Tin=80°F

outer convection heat transfer coefficient and wall thermal conductivity.

At the symmetry axis, the normal gradients of all dependent variables except the normal velocity component are set to zero and the normal velocity is taken to be zero (V = 0). No-slip boundary conditions are given to velocity components at the wall.

2.3. Solution Method

The discretization equations for the set of governing equations were derived using the implicit finite-difference method on meshes of orthogonally intersecting grid lines. This framework is the control volume approach developed by Patankar[11]. Staggered grids are employed in this approach for the velocity components to avoid wavy field of pressure distribution while power law formulation is employed to express the combined convective and diffusive fluxes across the boundaries of the control volume. The discretization equations were solved iteratively by line-by-line procedure of the tri-diagonal matrix algorithm, and the velocity-pressure link through the continuity equation is made by the SIMPLER algorithm[1].

Grid nodes were densely distributed along the boundaries (i.e., inlet, outlet, walls, insulation-condensate interface, condensate-steam interface) of the computational domain where steep variations are predicted to occur initially. Preliminary experiments and trial runs were conducted, and the resulting information was used to decide the number of grids for the final experiment. The grid distribution in the x and r direction is 50 and

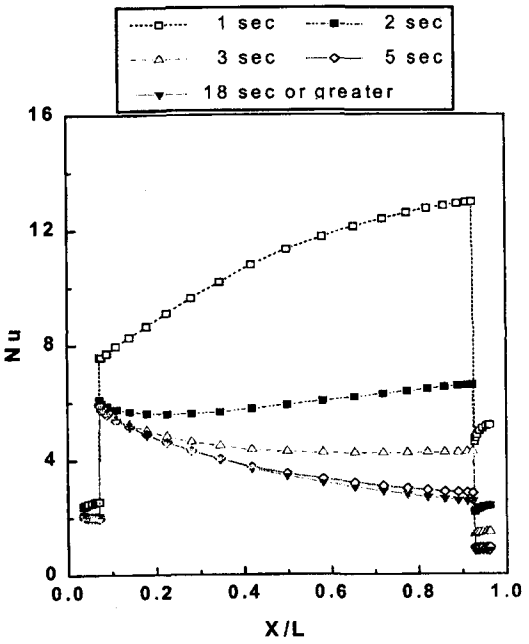

Fig. 5. Axial Distribution of Nusselt Number for Various Time Steps with Tin=120°F

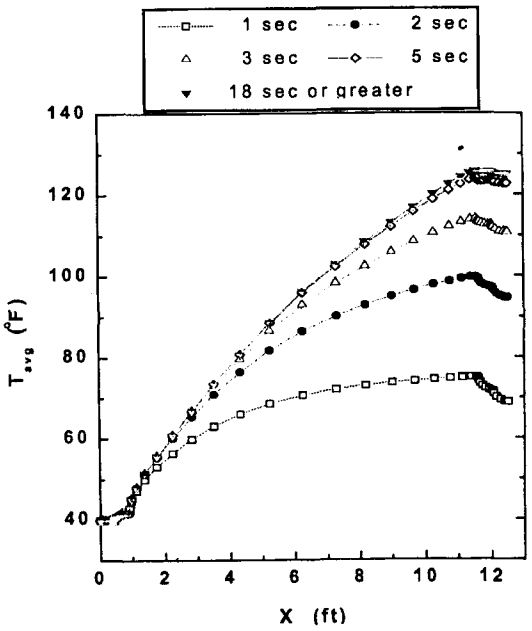

Fig. 6. Average Temperature Distribution for Various Time Steps with Tin=40°F

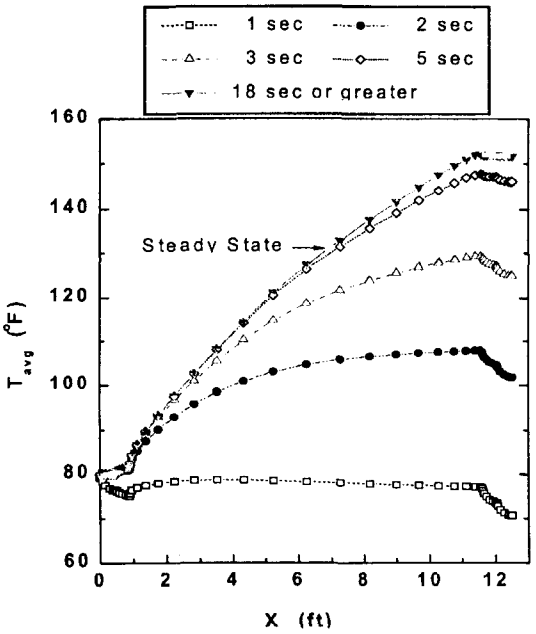

Fig 7. Average Temperature Distribution for Various Time Steps with Tin=80°F

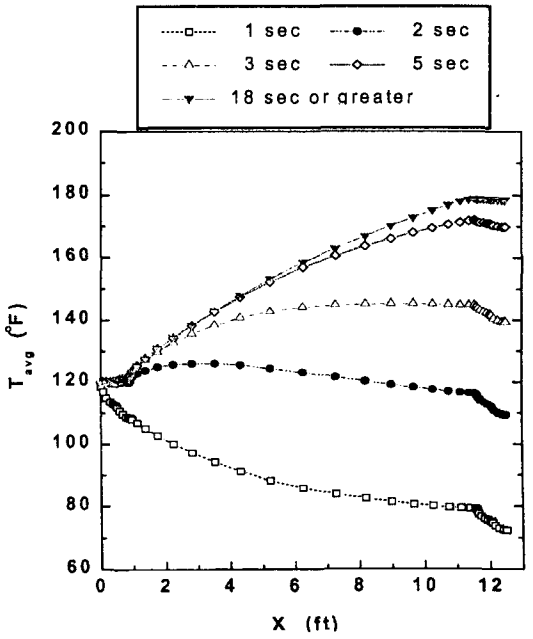

Fig. 8. Average Temperature Distribution for Various Time Steps with Tin=120°F

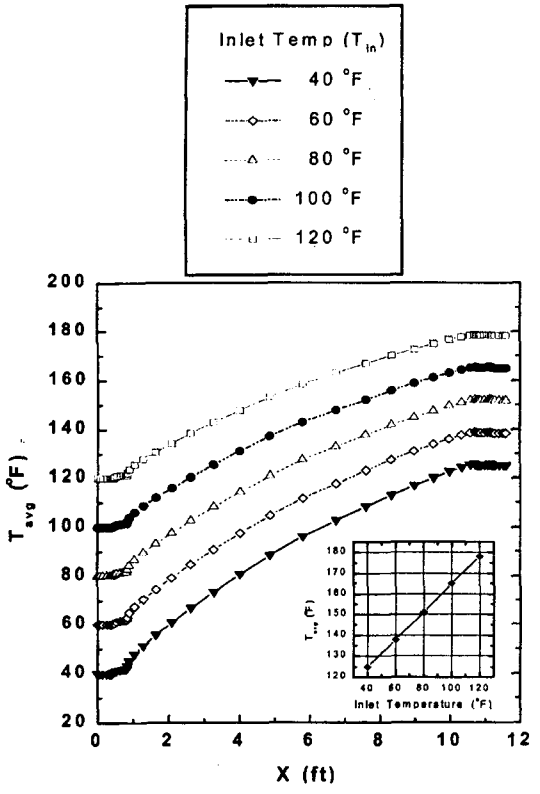

Fig. 9. Average Temperature Distribution at Steady State for Various Inlet Temperatures

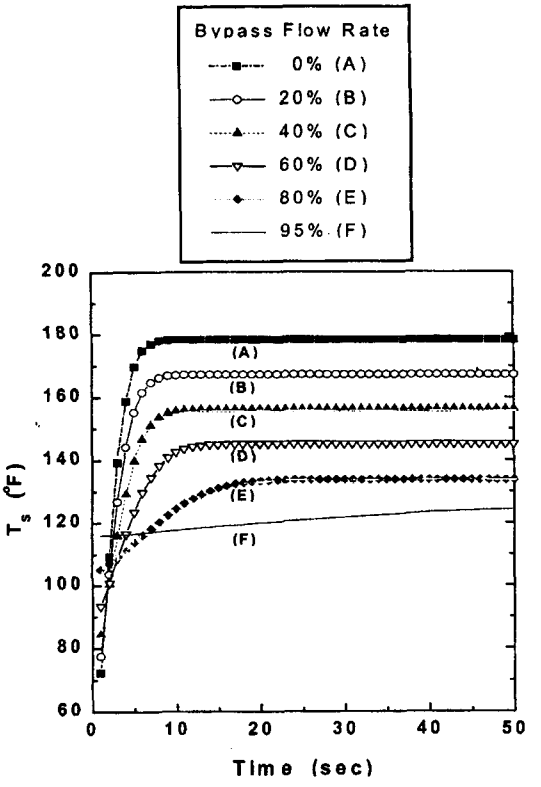

Fig. 10. Effects of Bypass Flow Rate on the Transient Seal Injection Temperature

30. In order to improve convergence, under-relaxation factors were used both for the velocity components and temperature. The optimum values of under-relaxation factors depend upon the nature of the problem, the number of grid points and the grid spacing. These values were found from exploratory computations. Typical values used were from 0.2 to 0.5 for the velocity components and 0.7 to 1.0 for the temperature. The converged solutions at each time step were assumed when relative errors of all variables between two successive iterations are less than 10^{-4}

The first time step was taken to be small (i.e., $\Delta t=1$ sec), while every subsequent interval was proportionally increased by 10% over the previous one. At the initial time steps, approximately 200 iterations were required to obtain converged solutions at each time step, and the iterations were significantly reduced with lapse of time, and when approaching steady state solutions, only 5-7 iterations were enough to obtain converged solutions.

3. Results and Discussion

The initial temperature was set at 40°F for all cases. Under this intial temperature, calculations were performed for the step change of inlet fluid temperatures in the range

of 40-120°F and inlet flow rates of 0-95%(bypass flow rate 95-0%). Actual design values were used for secondary temperature of seal injection heat exchanger (295°F) and outside heat transfer coefficients (condensate region: 300, steam region: 1574 Btu/h ft^2°F).[1]. Total pipe length of 11.3 ft is divided into two insulate sections(0.333 ft each), two condensate sections(0.333 ft each) and one steam section(9.94 ft).

Figs. 3, 4 and 5 show the axial distributions of Nusselt number at the wall-fluid interface without bypass flow for 5 different time steps and inlet temperatures of 40, 80 and 120°F, respectively.

Fig. 3 is the case when the inlet temperature is same as the initial temperature. It can be seen from Fig. 3 that Nusselt number upstream is significantly greater than that of downstream region, and right after a peak at the first condensate-steam interface, it drastically decreases with the axial direction and then monotonically decreases as approaches to the second steam-condensate interface. The Nusselt number also decreases with time until the steady state is reached. The results indicate that heat transfer during the initial transient period is primarily governed by the radial conduction mechanism, and heat transfer by axial convection and conduction effects increases with time. Fig. 4 represents Nusselt number distribution when the inlet temperature is greater than the initial temperature(T_{in}=80°F). At the initial transient (t<1sec), Nusselt number somewhat increases with the axial direction in the steam region. This is resulted from the temperature differences between the pipe fluid and the secondary fluid, in which the temperature difference becomes gradually higher along the axial direction compared to case of Fig. 3. As time passes(t>2sec), the temperature difference along the axial direction decreases due to heat transfer by axial convection and conduction, and thus Nusselt number distribution of Fig. 4 again appears to be similar to that of Fig. 3. This trend is more evidently seen from Fig. 5, which is the case when the inlet temperature is much higher than the initial temperature (T_{in}=120°F). At t<1 in Fig. 5, the axial distribution of Nusselt number obviously increases in the steam region, and decreasing rate after t>3 is clearly reduced, compared to the cases of Fig. 3 and Fig. 4. Note that the peak does not appear at the condensate-steam interface in Fig. 5.

Primary interest of this study is to investigate the exit temperature of the seal injection heat exchanger. Figs. 6, 7 and 8 represent the average temperature distributions for 5 subsequent time steps and for inlet temperatures of 40, 80 and 120°F. T_{in} = 40°F of Fig. 6, the average temperatures increase with the axial direction in steam region and increasing rates are higher near the entrance and with increasing time, but opposite trends occur in the second condensate region. This result is consistent with the Nusselt number distributions of Fig. 3, where heat transfer effects are dominant near the entrance, drastically decrease after a peak and gradually decrease downstream. When the inlet temperatures are increased(Figs. 7 and 8), the average temperatures decrease in the steam region at the initial time period, but after a certain time is passed, it tends to again increase.

Fig. 9 shows the axial distributions of average temperature inside the tube at the steady state for various inlet temperatures. The inserted graph in Fig. 9 represents the

Table 2. A Summary of Seal Injection Temperature and HX Exit Temperature at Steady State

T_{In}	Bypass Flow Rate									
	20%		40%		60%		80%		95%	
	T_{Out}	T_{Sum}	T_{Out}	T_{Sum}	T_{Out}	T_{Sum}	T_{Out}	T_{Sum}	T_{Out}	T_{Sum}
40	126	109	128	93	131	76	140	60	185	47
60	139	123	141	109	144	94	153	79	194	67
80	153	138	154	124	157	111	165	97	203	86
100	166	153	167	140	170	128	177	115	211	106
120	179	167	180	156	182	145	189	134	220	125

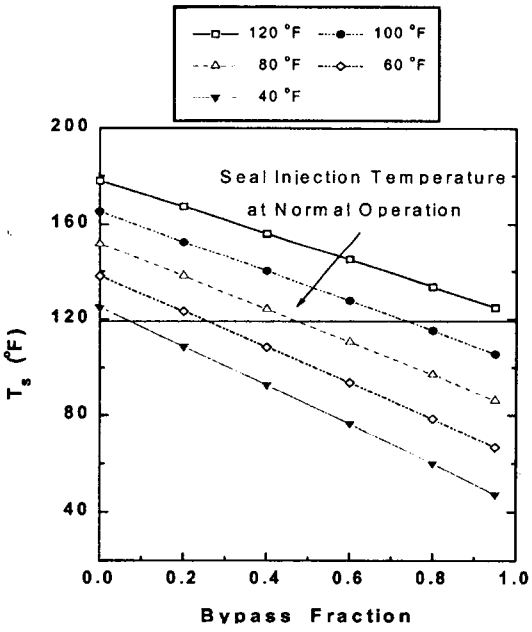

Fig. 11. Steady State Seal Injection Temperature for Various Inlet Temperatures and Bypass Flow Rates

exit temperature at the steady state. The average temperatures increase almost proportionally with the axial distance in the steam region, but nearly constant in the condensate region. As can be seen in the inserted graph of Fig. 9, except for the case of inlet temperature of 40°F, the exit temperature exceeds the design requirement of 125°F.

As stated previously, in order to maintain the exit temperature below the design limit of 125°F during transients, a bypass line is installed(Fig. 1). Fig. 10 presents the transient seal injection temperature distributions for various bypass flow rates with the step change of inlet temperature of 120°F. The seal injection temperature T_{Sum} is the temperature of the mixed fluids passing through the heat exchanger and the bypass flow, which is calculated by:

$$T_{Sum} = \frac{Q_{SIHX}}{Q_{Sum}} T_{out} + \frac{Q_{Bypass}}{Q_{Sum}} T_{in} \qquad (8)$$

where T_{in} is the inlet temperature, T_{out} is the exit temperature, Q_{SIHX} is the inlet flow rate, Q_{Bypass} is the bypass flow rate, and Q_{Sum} is the total flow rate of the mixed flow. As can be seen in Fig. 10, the seal injection temperatures abruptly increase with time during initial transients and increasing rates are more significant with smaller bypass flow rates. The time required to reach the steady

state becomes longer with increasing bypass flow rate. For the case of bypass flow rate of 95%, the seal injection temperature gradually and linearly increases and is the only case satisfying the design requirement of 125°F among test cases. A colligated result of steady state seal injection temperatures is shown in Fig. 11 and also summarized in Table 2 for various inlet temperatures and bypass flow rates. The seal injection temperatures decrease linearly with bypass flow rate, but almost proportionally increase with the inlet temperature. The conditions which satisfy the seal injection temperature requirement are the region below the horizontal line in Fig. 11 or in the shadowed area in Table 2.

4. Conclusions

Finite-difference technique was utilized for the investigation of transient heat transfer characteristics of the seal injection heat exchanger with a step change of inlet temperature. In order to reduce thermal transients of seal injection temperature, a bypass line is suggested to be installed around the seal injection heat exchanger, and its effects were also investigated in this study. Results indicate that when the inlet temperature is suddenly changed from the initial temperature, conduction in the radial direction is the governing heat transfer mechanism at the initial transient period, but as time passes axial convection and conduction effects are relatively increased and become an important heat transfer mechanism after a certain time. In most cases, the Nusselt numbers appear to be large near the entrance and have significant variations at the boundary interfaces. At the steady state, the seal injection temperatures linearly decrease with bypass flow rate, but almost proportionally increase with the inlet temperature. Seal injection temperatures which satisfy the design requirement of 125°F can be identified in this study, and among test cases, these temperatures are found in the range of higher bypass flow rates or lower inlet temperatures.

References

1. S. V. Patankar, "A Calculation Procedure for Two-Dimensional Elliptical Situation," *Numerical Heat Transfer*, **4**, 409 (1981).
2. H. T. Lin and Y. P. Shih, "Unsteady Thermal Entrance Heat Transfer of Power-Law Fluids in Pipes and Plate Slits," *Int. J. Heat Mass Transfer*, **24**, 1531 (1981).
3. H. T. Lin, K. H. Hawks and W. Leidenfrost, "Unsteady Thermal Entrance Heat Transfer in Laminar Pipe Flows with Step Change in Ambient Temperature," *Warme-Stoffuertragung*, **17**, 125 (1983).
4. R. M. Cotta, M. N. Ozisik and D. S. McRac, "Transient Heat Transfer in Channel Flow with Step Change in Inlet Temperature," *Numerical. Heat Transfer*, **9**, 619 (1986).
5. J. Sucec, "An Improved Quasi-Steady Approach for Transient Conjugated Forced Convection Problems," Int. *J. Heat Mass Transfer*, **24**, 1711 (1981).
6. J. Sucec and A. M. Sawant, "Unsteady, Conjugated, Forced Convection Heat Transfer in a Parallel Plate Duct," *Int. J. Heat Mass Transfer*, **27**, 95 (1984).
7. J. Sucec, "Unsteady Conjugated Forced Heat Transfer in a Duct with Convection from the Ambient," *Int. J. Heat Mass Transfer*, **30**, 1963 (1987).
8. T. F. Lin and J. C. Kuo, "Transient

Conjugated Heat Transfer in Fully Developed Laminar Pipe Flows," *Int. J. Heat Mass Transfer*, **31**, 1093 (1988).
9. K. T. Lee and W. M. Yan, "Transient Conjugated Forced Convection with Fully Developed Laminar Flow in Pipes," *Numerical Heat Transfer*, **23**, 341 (1993).
10. T. Cebeci and A. M. O. Smith, Analysis of Turbulent Boundary Layers, Ser. in Math. & Mech. Vol. XV, Academic Press (1974).
11. S. V. Patankar, Numerical Heat Transfer and Fluid Flow, Hemisphere, Washington D. C. (1980).